

Green Tea Epigallocatechin-3-Gallate Mediates T Cellular NF- κ B Inhibition and Exerts Neuroprotection in Autoimmune Encephalomyelitis¹

Orhan Aktas,^{2*} Timour Prozorovski,^{2*} Alina Smorodchenko,^{2*} Nicolai E. Savaskan,[†] Roland Lauster,[‡] Peter-Michael Kloetzel,[§] Carmen Infante-Duarte,^{*} Stefan Brocke,[¶] and Frauke Zipp^{3*}

Recent studies in multiple sclerosis and its animal model, experimental autoimmune encephalomyelitis (EAE), point to the fact that even in the early phase of inflammation, neuronal pathology plays a pivotal role in the sustained disability of affected individuals. We show that the major green tea constituent, (–)-epigallocatechin-3-gallate (EGCG), dramatically suppresses EAE induced by proteolipid protein 139–151. EGCG reduced clinical severity when given at initiation or after the onset of EAE by both limiting brain inflammation and reducing neuronal damage. In orally treated mice, we found abrogated proliferation and TNF- α production of encephalitogenic T cells. In human myelin-specific CD4⁺ T cells, cell cycle arrest was induced, down-regulating the cyclin-dependent kinase 4. Interference with both T cell growth and effector function was mediated by blockade of the catalytic activities of the 20S/26S proteasome complex, resulting in intracellular accumulation of I κ B- α and subsequent inhibition of NF- κ B activation. Because its structure implicates additional antioxidative properties, EGCG was capable of protecting against neuronal injury in living brain tissue induced by *N*-methyl-D-aspartate or TRAIL and of directly blocking the formation of neurotoxic reactive oxygen species in neurons. Thus, a natural green tea constituent may open up a new therapeutic avenue for young disabled adults with inflammatory brain disease by combining, on one hand, anti-inflammatory and, on the other hand, neuroprotective capacities. *The Journal of Immunology*, 2004, 173: 5794–5800.

Tea (*Camellia sinensis*) and its constituent polyphenols have been reported to possess anticarcinogenic properties in a wide variety of experimental systems in vitro and in vivo. Drinking tea, especially green tea, is associated with a lower incidence of human cancer (1, 2). Subsequent studies demonstrated that certain fractions of green tea, among them (–)-epigallocatechin-3-gallate (EGCG),^{3,4} promote apoptosis and cell cycle arrest of transformed cells (3–5). Moreover, immunomodulatory properties of green tea extracts such as inhibiting endotoxin-induced TNF- α production (6) and neutrophil-mediated effects have been recently described (7). In a mouse model of stroke, a neuroprotective role was observed (8) and linked in a Parkinson's dis-

ease model to regulation of superoxide dismutase and catalase activity in the brain (9).

Multiple sclerosis (MS) is a multiphasic autoimmune disease of the CNS (10) in which myelin-specific CD4⁺ Th1 cells are thought to orchestrate the effector processes resulting in the destruction of the myelin sheath (11). Recent studies in MS and its animal model, experimental autoimmune encephalomyelitis (EAE) (12), suggest that already during the early phase of inflammation, neuronal pathology involving axonal transection and loss of parental cell bodies plays a pivotal role in disease severity (13, 14). It has become evident that long-term disability in MS correlates better with axonal damage than with the degree of demyelination (13, 14). We have very recently unraveled a process linking demyelination and neuronal damage (15). As a consequence of demyelination, the myelin breakdown product 7-ketocholesterol, which can be detected in the cerebrospinal fluid of MS patients, induces microglia-mediated apoptotic cell death of neurons in the brain stem motor region (15). However, currently approved therapies, which have to be administered parenterally in young disabled adults with neuroinflammatory disorder, primarily focus on the inflammatory aspect of the CNS disease (16), are only partly effective, and are often limited by side effects. In contrast, neuroprotective agents have not yet been established in this autoimmune disorder. In light of the pharmacological profile of EGCG, and its reported properties in immunity and neurodegeneration, we hypothesized a potential beneficial role of EGCG in the treatment of neuroinflammation and subsequently discovered the underlying mechanisms of action.

Materials and Methods

Induction, treatment, and evaluation of EAE

Female SJL/J mice (6–8 wk; ~20 g body weight; Charles River Laboratories, Sulzfeld, Germany) were immunized s.c. with 75 μ g of proteolipid

*Institute of Neuroimmunology, Neuroscience Research Center, Charité, Berlin, Germany; [†]Division of Cellular Biochemistry, The Netherlands Cancer Institute, Amsterdam, The Netherlands; [‡]German Arthritis Research Center, Berlin, Germany; [§]Institute of Biochemistry, Charité, Berlin, Germany; [¶]Experimental Pathology, Department of Pathology, Hebrew University, Hadassah Medical School, Jerusalem, Israel

Received for publication March 29, 2004. Accepted for publication August 26, 2004.

The costs of publication of this article were defrayed in part by the payment of page charges. This article must therefore be hereby marked *advertisement* in accordance with 18 U.S.C. Section 1734 solely to indicate this fact.

¹ This work was supported by grants from the Bundesministerium für Bildung und Forschung, the Gemeinnützige Hertie-Stiftung, and the Deutsche Forschungsgemeinschaft (SA 1041/3-1).

² O.A., T.P., and A.S. contributed equally to this work.

³ Address correspondence and reprint requests to Dr. Frauke Zipp, Institute of Neuroimmunology, Neuroscience Research Center, NWFZ 2680, Charité, 10098 Berlin, Germany. E-mail address: frauke.zipp@charite.de

⁴ Abbreviations used in this paper: EGCG, (–)-epigallocatechin-3-gallate; NMDA, *N*-methyl-D-aspartate; BSO, buthionine sulfoximine; MS, multiple sclerosis; TCL, T cell line; ROS, reactive oxygen species; EAE, experimental autoimmune encephalomyelitis; CDK, cyclin-dependent kinase; PLP, proteolipid protein; MBP, myelin basic protein; APP, amyloid precursor protein.

protein (PLP) peptide p139–151 (purity >95%; Pepceuticals, Leicester, UK) in a 0.2-ml emulsion consisting of equal volumes of PBS and CFA (Difco, Franklin Lakes, NJ) and containing 6 mg/ml *Mycobacterium tuberculosis* H37Ra (Difco). *Bordetella pertussis* toxin (200 ng; List Biological Laboratories, Campbell, CA) was administered i.p. at days 0 and 2. For treatment, EGCG (Sigma-Aldrich, St. Louis, MO) was dissolved in 0.9% NaCl. EGCG or vehicle (0.9% NaCl) were administered by gavage (100 μ l per mouse) twice daily. Mice were scored as follows: 0, no disease; 1, tail weakness; 2, paraparesis; 3, paraplegia; 4, paraplegia with forelimb weakness; and 5, moribund or dead animals (17). All procedures were conducted according to protocols approved by the local animal welfare committee.

Proliferation and apoptosis

Human CD4⁺ T cell lines (TCLs) specific for human myelin basic protein (MBP; FN8 and MA14) or birch pollen (SW21) were established with a modified "split-well" protocol as previously described (17). For proliferation, 0.7×10^5 cells were stimulated with 2×10^5 autologous-irradiated (3000 rad) PBMC as APCs and Ag, or with anti-CD3 (OKT3; coated at 1 μ g/ml; American Type Culture Collection, Manassas, VA) and 2.5 μ g/ml anti-CD28 (R&D Systems, Minneapolis, MN), respectively. For murine bulk cell cultures, cell suspensions from draining lymph nodes were stimulated in 96-well microtiter plates (2×10^5 cells/well) with peptide. [³H]Thymidine incorporation (0.5 μ Ci/well; Amersham Biosciences, Piscataway, NJ) was measured 72 h after stimulation with Ag and 48 h with anti-CD3/CD28. Radioactivity was detected using a MicroBeta beta counter (PerkinElmer, Wellesley, MA) after 18 h. For apoptosis, DNA fragmentation of susceptible Jurkat T cells was determined by flow cytometry of hypodiploid DNA as described previously (17).

Immunohistochemistry

Spinal cords and brain stems from mice transcardially perfused with 4% paraformaldehyde were postfixed overnight. Vibratome sections (Thermo Shandon, Pittsburgh, PA) were stained with H&E and evaluated in a blinded manner for inflammation as calculated by number of inflammatory foci (four ocular fields per section and six mice per group) (17). For caspase 3 and β -amyloid precursor protein (β -APP) staining, sections were quenched using 3% H₂O₂, washed, and blocked (10% NGS, 0.5% Triton X-100) before overnight incubation with anti-active caspase 3 (1:100; R&D Systems) and anti- β -APP (1:1000; Zymed Laboratories, San Francisco, CA). Sections were immunolabeled and developed using the avidin: biotinylated enzyme complex technique (ABC-Elite; Vector Laboratories, Burlingame, CA). Neurons positive for active caspase 3 were counted in brain stem sections (four ocular fields per section and six mice per group) (15).

Flow cytometry

Single-cell suspensions were prepared from draining lymph nodes, and a portion was stained with anti-CD25-APC (BD Pharmingen, San Jose, CA). Before staining, cells were incubated with anti-CD14/CD32 (BD Pharmingen) to prevent unspecific Ab binding. For intracellular staining, cells were activated for 4 h (5 ng/ml PMA, 1 μ g/ml ionomycin), and brefeldin A (5 μ g/ml) was added for the last 2 h. Cells were fixed, permeabilized with FACS buffer containing saponin (PBS, 0.5% saponin, 0.5% BSA, 0.1% Na₂S₂O₃), stained with anti-IFN- γ -PE/TNF- α -APC/IL-4-APC Abs (BD Pharmingen), and analyzed on a FACSCalibur using CellQuest software (BD Pharmingen).

Western blot

Cells were washed with PBS and resuspended in lysis buffer (10 mM Tris, 150 mM NaCl, 5 mM EDTA, 1% Triton X-100, 1 mM DTT, 0.2 mM PMSF, 1 μ g/ml aprotinin, 1 μ g/ml pepstatin, 0.5 μ g/ml leupeptin). Total protein (30 μ g/ml per lane) was separated by 10% SDS-PAGE. After transfer, blots were incubated with anti-I κ B- α (Chemicon International, Temecula, CA), anti-cyclin-dependent kinase (CDK4; Santa Cruz Biotechnology, Santa Cruz, CA), anti-p27^{Kip1} (Santa Cruz Biotechnology), or anti-ubiquitin (Sigma-Aldrich) following HRP-conjugated secondary Ab (DakoCytomation, Carpinteria, CA) and ECL system (Amersham Biosciences) as described (18).

Brain slice cultures

Organotypic entorhinal-hippocampal slice (350 μ m thick) cultures from 10-day-old SJL mice were prepared on a tissue chopper (Bachhofer) and cultured as described (19). Neuronal cell death was induced with recombinant TRAIL and *N*-methyl-D-aspartate (NMDA; Sigma-Aldrich) after 24 h. For TRAIL production, N-terminal truncated human TRAIL (residues 95–281) containing an N-terminal 6-His tag was expressed in *Escherichia coli* BL21 cells. After purification on Ni²⁺-nitrilotriacetate-agarose (Clontech Laboratories, Palo Alto, CA), untagged proteins were dialyzed against PBS. Damage in brain slices was detected by addition of 5 μ g/ml propidium iodide (30 min at 36°C). Slices were examined using a rhodamine filter (488 nm/515 nm) with a dark-field inverse fluorescence microscope (Olympus, Melville, NY). For resectioning, slices were immersed before the preparation of 18- μ m thin horizontal cryostat sections, and quantification of PI⁺ cells was conducted as previously described (15).

erichia coli BL21 cells. After purification on Ni²⁺-nitrilotriacetate-agarose (Clontech Laboratories, Palo Alto, CA), untagged proteins were dialyzed against PBS. Damage in brain slices was detected by addition of 5 μ g/ml propidium iodide (30 min at 36°C). Slices were examined using a rhodamine filter (488 nm/515 nm) with a dark-field inverse fluorescence microscope (Olympus, Melville, NY). For resectioning, slices were immersed before the preparation of 18- μ m thin horizontal cryostat sections, and quantification of PI⁺ cells was conducted as previously described (15).

HT22 neuronal cell culture assays

For assessment of viability, hippocampal HT22 cells (20) were seeded at 5000 neurons per well in 96-well plates and cultured for 16 h. On the following day, cells received fresh medium and were incubated with EGCG 2 h before incubation with TRAIL with and without cycloheximide (CHX; 0.5 μ g/ml). Crystal violet assay was performed 16 h thereafter as previously described (21). Briefly, cells were stained for 30 min with 0.5% crystal violet in 20% methanol. After washing and drying, crystal violet was dissolved in 50 ml/well of 0.1 M sodium citrate solution diluted in 50% ethanol and subsequently quantified photometrically by absorbance at 550 nm (Dynatech Laboratories, Chantilly, VA). Values are expressed as the percentage of survival compared with untreated controls. Total protein extracts for immunoblots were prepared similarly. For detection of intracellular peroxides, intracellular accumulation of reactive oxygen species (ROS) was induced by 100 μ M buthionine sulfoximine (BSO) in HT22 cells (20). Cells were incubated with 10 μ M 5-carboxy-2',7'-dichlorodihydrofluorescein diacetate (DCFDA; Molecular Probes, Eugene, OR) for 30 min at 37°C. Wells without cells were loaded with DCFDA serving as negative controls. Fluorescence measurements were made on a Fluorostar platereader (SLT Labinstruments) at E_x λ 488 nm and E_m λ 530 nm.

Statistics

For group comparisons, the Mann-Whitney *U* test was applied. For EAE courses, ANOVA with Bonferroni adjustment was performed as previously described (17).

Results

Green tea polyphenol EGCG prevents and reverses disability in autoimmune encephalomyelitis

As a first step, we explored the therapeutic effect of the green tea polyphenol EGCG in EAE. This polyphenol was chosen because it is easily absorbed from the digestive tract and penetrates the brain, reaching levels similar to those found in lung, liver, kidney, and other organs (22). SJL/J mice were started on oral therapy with EGCG (300 μ g per mouse in 0.9% NaCl) or vehicle (0.9% NaCl) twice daily at the time of immunization with PLP p139–151, resulting in relapsing-remitting EAE (17). EGCG treatment enhanced animals' recovery from disease manifestation and significantly protected them from long-term neurological deficits, as indicated by the mean clinical scores over an observation period up to 131 days (Fig. 1A). EGCG administration started at the onset of acute disease prevented mice from relapses and prolonged neurological sequelae during subsequent relapse with a maximum disease score of 1.4 ± 0.3 in the EGCG group vs 2.7 ± 0.5 in the vehicle group ($p < 0.05$) and significantly lower mean clinical disease scores (Fig. 1B). The therapeutic effect of oral EGCG was found to be dose-dependent: a dose of 60 μ g per mouse (administered twice daily) was sufficient to attenuate the course of EAE, whereas a lower dosage (12 μ g per mouse twice daily) was not (Fig. 1C). Histological examination revealed large inflammatory lesions throughout the brain stem and spinal cord in vehicle-treated mice, while EGCG-treated animals showed significantly reduced inflammation (Fig. 2A).

Analysis of the T cell response

To unravel the underlying mechanisms, we next examined T cell response *ex vivo*. Draining lymph node cells from immunized animals treated with EGCG for 10 days exhibited a markedly lower proliferative response to the encephalitogenic PLP p139–151 peptide than control animals (Fig. 2B). Further, oral EGCG led to a

FIGURE 1. Oral EGCG therapy inhibits and reverses relapsing-remitting EAE. **A**, For the preventive treatment paradigm, EGCG (●, 300 μg per mouse twice daily) or vehicle (○, NaCl 0.9%) was orally administered from the day of immunization on. Disease severity was significantly reduced in the EGCG group (*, $F_{31-131}(1,101) = 6.7$, $p < 0.05$; ANOVA; $n = 6$ per group). **B**, For treatment of established disease, mice were randomized into 2 groups after disease manifestation on day 12 and subsequently received either oral EGCG or vehicle. Clinical disease was significantly reduced in the EGCG group (*, $F_{50-75}(1,26) = 4.9$, $p < 0.05$; ANOVA; $n = 9$ per group). **C**, Dose titration experiments showed that 60 μg of EGCG per mouse administered twice daily attenuated EAE (●), as compared with the vehicle control group (○; *, $F_{10-16}(1,7) = 5.0$, $p < 0.05$; ANOVA, $n = 8$ per group). In contrast, a lower dose (12 μg of EGCG per mouse administered twice daily; ▲) had no significant effect.

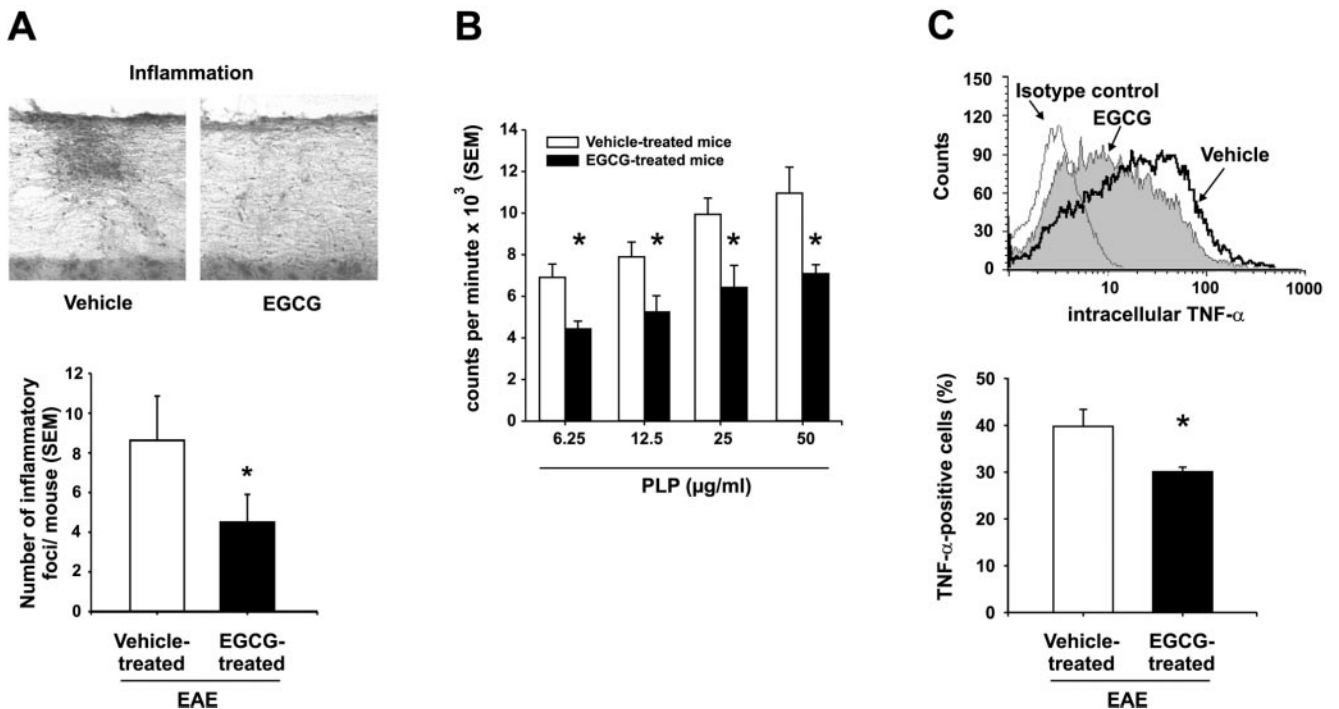
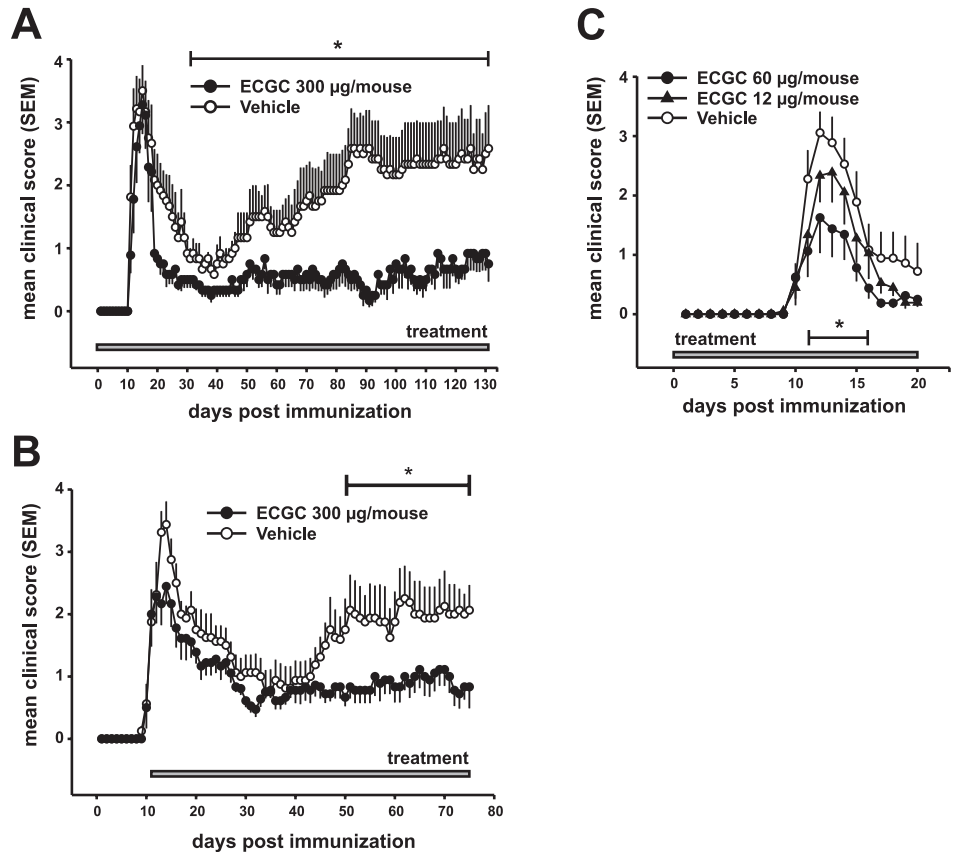


FIGURE 2. EGCG inhibits myelin-specific inflammatory responses. **A**, Representative H&E staining of spinal cord longitudinal sections from EAE in Fig. 1A. Number of inflammatory foci in the brain stem and spinal cord was assessed. **B** and **C**, Four mice per group received EGCG (filled bars) or vehicle (open bars) from day 1 after immunization. Ten days later, lymph node cells were assessed for proliferation in response to PLP (**B**) or TNF- α synthesis (**C**). The upper graph in **C** is a representative flow cytometry histogram. The thick bold line represents the staining of cells from vehicle-treated animals; the thin line with gray shading below represents the staining of cells from EGCG-treated animals; the thin line without shading represents the staining of cells from isotype controls (see labels). The lower graph shows the percentage of TNF- α -positive cells (open bars, vehicle-treated group; filled bars, EGCG-treated group). Data show mean \pm SEM; *, $p < 0.05$.

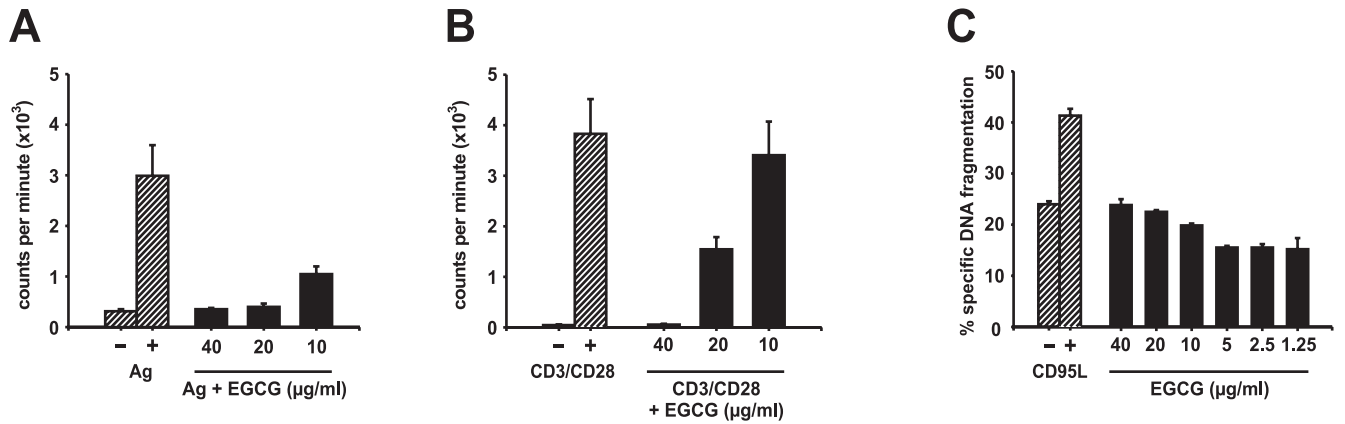


FIGURE 3. EGCG inhibits human Ag-specific CD4⁺ T cell proliferation. *A*, Proliferation of the human MBP-specific TCL FN8 stimulated with (+) or without (-) Ag presented by irradiated autologous APCs. *B*, The same TCL was stimulated with (+) or without (-) anti-CD3/CD28 Abs. *C*, Specific DNA fragmentation was assessed in Jurkat T cells incubated with murine CD95 ligand (10 U/ml) as positive control or EGCG, respectively.

reduction in TNF- α synthesis, demonstrated by intracellular FACS staining *ex vivo* (Fig. 2C). In contrast, expression of IL-4 or IFN- γ was unaffected. There was no link between successful EAE therapy and expansion of regulatory T cells, determined by comparable fractions of CD4⁺CD25⁺ cells in EGCG- and vehicle-treated animals (data not shown). Similarly, EGCG treatment did not affect the proportion of CD4/CD8 cells.

EGCG inhibits T cell proliferation by suppressing CDK4 and up-regulating I κ B- α

In human CD4⁺ Th1 MBP-specific T cells, EGCG, in a dose-dependent manner, blocked expansion of cells stimulated with peptide-loaded autologous APCs (Fig. 3A) and cells proliferating in response to direct TCR engagement by anti-CD3/CD28 stimulation (Fig. 3B). The micromolar EGCG concentrations used in this and the following *in vitro* assays are likely to be achieved in humans, as indicated by previous investigations (23). Interestingly, no indication of EGCG-mediated T cell death was observed with trypan blue exclusion assay (data not shown). Even in apoptosis-

susceptible Jurkat T cells, no DNA fragmentation was induced (Fig. 3C), excluding a direct death-promoting role for EGCG in T cells. Western blot analysis showed that inhibition of the T cell proliferation by EGCG can be explained by interference on the cell cycle level, down-regulating expression of the CDK4. This effect was not mediated by p27^{kip1}, a CDK inhibitor and negative cell cycle regulator (Fig. 4A). In contrast, we observed that EGCG interfered with NF- κ B activation. While in untreated human T cells the crucial NF- κ B-inhibitor I κ B- α (24) was down-regulated upon stimulation, EGCG inhibited this pathway in a dose-dependent manner, resulting in an intracellular accumulation of I κ B- α (Fig. 4B). Further, TNF- α stimulation of T cells resulted in a strong degradation of I κ B- α within a few hours (Fig. 4C), which was completely reversed in the presence of EGCG. Since degradation of I κ B- α , a prerequisite of NF- κ B activity, is mediated by the cytosolic proteasome complex (24), intracellular accumulation of I κ B- α by EGCG may originate from inhibition of proteasome activity. This assumption was supported by a similar I κ B- α accumulation pattern in T cells in the presence of the synthetic 26S

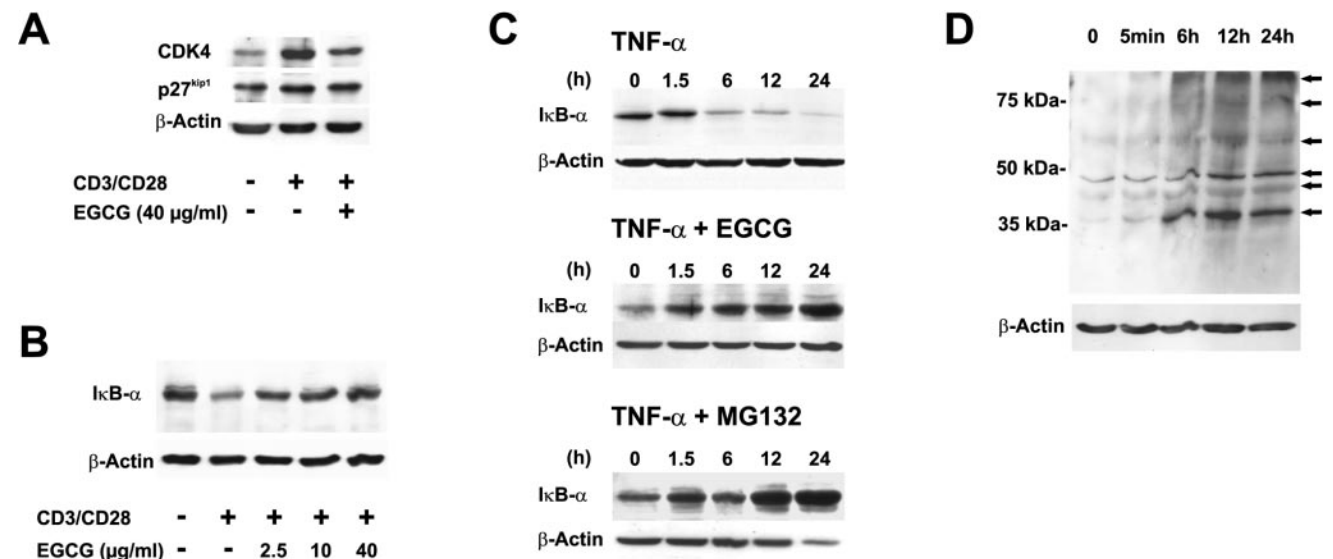


FIGURE 4. EGCG interferes with cell cycle, NF- κ B activation, and proteasome in CD4⁺ T cells. *A*, Human TCL MA14 was assessed for CDK4 and p27^{kip1} protein levels 24 h after anti-CD3/CD28 stimulation. *B*, The same TCL stimulated with anti-CD3/CD28 was used to analyze the NF- κ B inhibitor I κ B- α protein regulation by EGCG. *C*, Human TCL SW21 was cotreated with TNF- α (20 ng/ml) without (*upper panel*) or with EGCG (40 µg/ml; *middle panel*) or with proteasome inhibitor MG132 (10 µM; *bottom panel*) for indicated time periods. *D*, Accumulation of ubiquitinated proteins (arrows) in human TCL after stimulation with TNF- α (20 ng/ml) in the presence of EGCG (40 µg/ml).

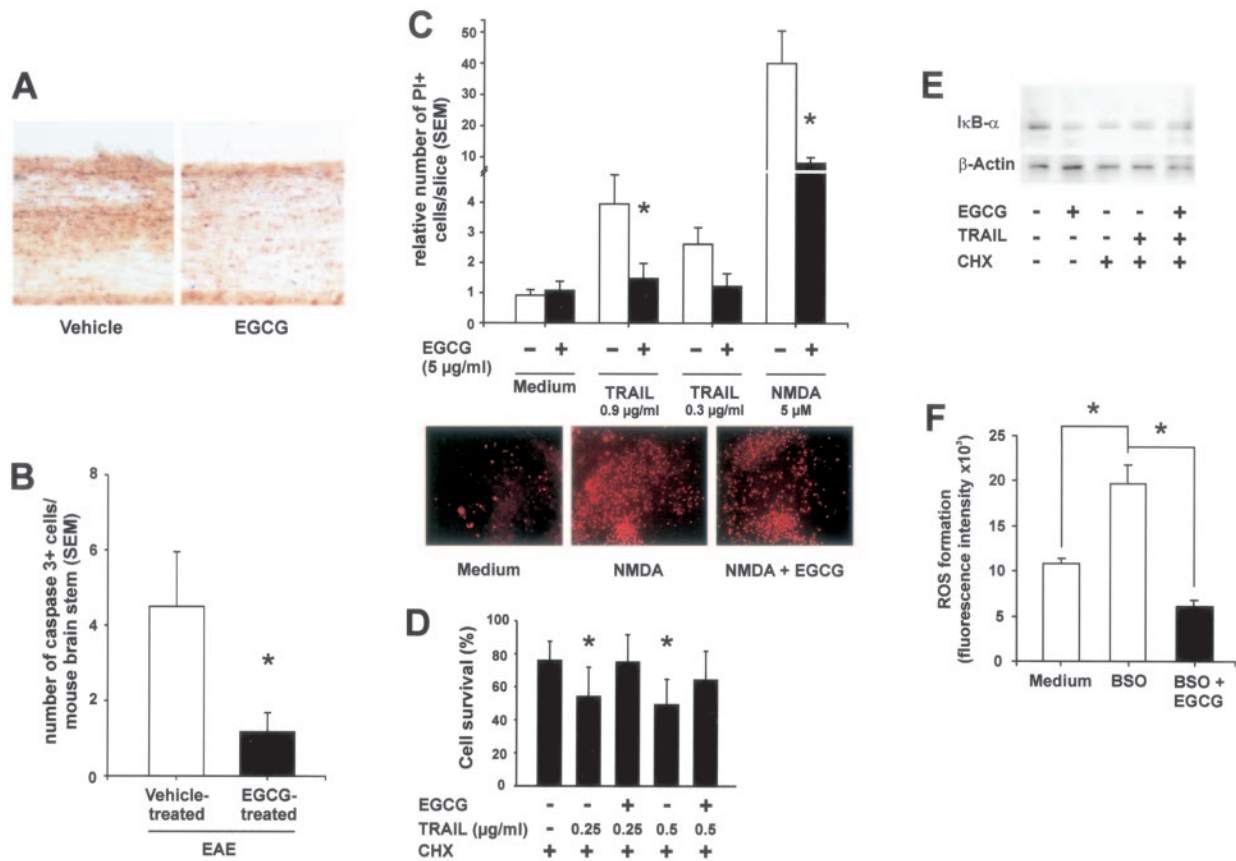


FIGURE 5. Neuroprotective effects of EGCG; reduced formation of ROS. *A*, Representative APP stainings of spinal cord longitudinal sections from EAE in Fig. 1*A*. *B*, Average number of active caspase 3-immunoreactive neurons in transverse brain stem sections ($n = 6$ per group). *C*, Living SJL brain slices ($n = 18$ per group) were exposed to TRAIL or NMDA. Results indicate mean cell counts in relation to nondamaged brain tissue (control = 1). Representative slices treated with NMDA without and with EGCG are shown. *D*, Survival of HT22 hippocampal neurons was determined in a crystal violet assay after incubation with different concentrations of TRAIL in the presence of CHX (0.5 $\mu\text{g/ml}$). EGCG was added at a concentration of 10 $\mu\text{g/ml}$. *E*, Western blot analysis for I κ B- α is shown in HT22 neurons, pretreated for 2 h with EGCG (10 $\mu\text{g/ml}$) and thereafter with TRAIL (1 $\mu\text{g/ml}$) in the presence of CHX (0.5 $\mu\text{g/ml}$) for 16 h. *F*, HT22 neurons were treated with 100 μM BSO, and simultaneously incubated with and without EGCG (5 $\mu\text{g/ml}$). Glutathione depletion induces ROS formation (mean \pm SD), which is prevented in the presence of EGCG. *, $p < 0.05$.

proteasome inhibitor MG132 (Fig. 4*C*). Indeed, the rapid increase in ubiquitinated proteins, the substrates of the proteasome complex, confirmed the involvement of proteasome inhibition in T cells by EGCG (Fig. 4*D*).

EGCG directly inhibits neuronal cell death by interference with ROS formation

Considering the reported effects of green tea compounds in neurodegenerative models, we analyzed whether the therapeutic efficacy of EGCG in EAE involves protection against neuronal damage. Indeed, we found reduced axonal pathology in EGCG-treated animals in the chronic phase (Fig. 5*A*). Quantitative analysis of caspase 3-positive neurons, shown to be present in the brain stem motor area of mice suffering from EAE (15), revealed significantly fewer apoptotic neurons in EGCG-treated as compared with vehicle-treated animals (Fig. 5*B*). Accordingly, we observed similar effects of EGCG on neurons in living organotypic hippocampal brain slice cultures from SJL/J mice, a system in which neurons can be maintained in an *in vivo*-like fashion (19). Damage was induced by exposing slices to neurotoxic NMDA and the apoptosis ligand TRAIL, which is reported to have neurotoxic properties (25) and involve the activation of NF- κ B (26). In both constellations, preincubation with EGCG 3 h before damage significantly

protected against neuronal cell death (Fig. 5*C*). Next, to unravel the underlying mechanisms, we investigated the impact of EGCG on HT22 hippocampal neurons. As in slices, TRAIL induces cell death in HT22 neurons which can be inhibited by EGCG (Fig. 5*D*). However, in contrast to our findings in T cells (Fig. 4*B*), no accumulation of I κ B- α was observed (Fig. 5*E*). Therefore, we hypothesized that due to its structure containing two trihydroxybenzoyl groups, EGCG may exert its neuroprotective activity directly as a free radical scavenger (27). In fact, we could show in a model of glutathione depletion-induced neurotoxicity (20) that EGCG is able to inhibit the formation of ROS in neurons. HT22 neurons were incubated with BSO, an inhibitor of glutathione synthetase, thereby inducing glutathione depletion, which subsequently results in neuronal cell death. Treating HT22 neurons with BSO induced a 2-fold increase in ROS, which could be prevented by EGCG application (Fig. 5*F*). These results demonstrate that EGCG acts downstream of glutathione synthetase and, therefore, directly targets ROS formation.

Discussion

We have shown that orally applied EGCG, the major polyphenolic compound of green tea, suppressed inflammation *in vivo*, inhibiting proliferation and TNF- α synthesis of T cells, and effectively

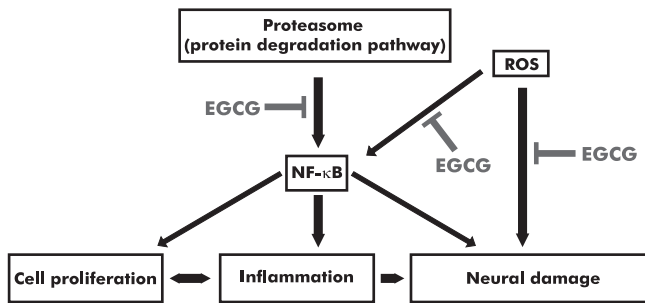


FIGURE 6. Proposed model for signal transduction pathways modified by EGCG. EGCG is capable of inhibiting both catalytic activities of the proteasome, including NF- κ B activation, and the amount of ROS. In lymphocytes, this leads to decreased proliferation and production of the proinflammatory cytokine TNF- α , while in neurons, it results in less damage. Additionally, the antioxidative effects of EGCG on neurons might involve the NF- κ B pathway as well, since ROS can induce NF- κ B, which regulates the expression of a variety of molecules contributing to cell proliferation, inflammation, and neuronal damage.

protected against relapsing CNS autoimmune disease, resulting in a favorable long-term clinical outcome. The human dosage equivalent of the most effective EGCG concentration tested here is contained in ~ 3 liters of conventionally brewed green tea. Recently, it was reported in collagen-induced experimental arthritis that application of unpurified green tea extracts reduced anti-collagen Ig levels and the expression of the proinflammatory cytokines TNF- α and IFN- γ in arthritic joints (28). Our data provide a mechanistic basis, demonstrating for the first time that the anti-inflammatory properties of EGCG are mediated by down-regulating NF- κ B in T cells. This transcription factor, crucial for the development of autoimmune encephalomyelitis (29), regulates the expression of genes encoding proinflammatory cytokines, chemokines, immune receptors, and adhesion molecules that play a key part in the initial recruitment of leukocytes to sites of inflammation (24). EGCG inhibited the catalytic activity of the proteasome in activated T cells, resulting in the intracellular accumulation of ubiquitinated proteins including the NF- κ B-suppressor I κ B- α . Supporting our conclusion that EGCG acts at the proteasome level, *in vitro* experiments showed that EGCG inhibited the proteolytic activities of both 20S and 26S proteasome complexes in the presence of Mg²⁺ (data not shown). While the proteasome complex plays a pivotal role in regulating T cell expansion (30), the overexpression of I κ B- α is known to suppress proliferation by inhibiting the G₁/S transition (31). Indeed, we found that EGCG directly induced T cell cycle arrest in the G₁/S transition phase, reducing CDK4 expression. We further detected reduced axonal pathology and fewer neurons eventually undergoing cell death in animals with chronic autoimmune encephalomyelitis, revealing an additional mechanism underlying the therapeutic potential of EGCG. The lack of I κ B- α accumulation in EGCG-treated neurons indicates that the neuroprotective effect of this polyphenol is mediated by interference with a distinct pathway which differs from the EGCG target in T cells. In fact, we could show a ROS-blocking capacity of EGCG in neurons, providing evidence for the concept that, as the structure of EGCG contains a polyphenol ester bond (32) and two trihydroxybenzoyl groups, both inhibition of catalytic activities of the proteasome and antioxidative properties of EGCG contribute to the therapeutic effects observed *in vivo*. ROS not only represent a supposed damage process in neurodegeneration, but also in neuroinflammation such as EAE (33).

MS is a multiphasic autoimmune CNS disease, involving injury to neuronal structures, including axons and parent cell bodies.

Since the available treatment only consists of immunomodulatory agents, green tea compounds such as epigallocatechin-3-gallate are candidates for the treatment of MS patients, as they are administered orally, are well tolerated (34), and exhibit synergistic beneficial effects, unraveled here, in disorders with both pathological elements, inflammation and neuronal injury (Fig. 6). One may speculate that the biological properties described here contribute to the lower prevalence rates of MS in Asian populations with traditional consumption of green tea (35).

Acknowledgments

We thank B. Seeger, N. Nowakowski, and O. Riede for technical assistance, and K. Rosegger and A. Mason for carefully reading the manuscript as native speakers.

References

- Mukhtar, H., and N. Ahmad. 1999. Green tea in chemoprevention of cancer. *Toxicol. Sci.* 52:111.
- Suganuma, M., S. Okabe, N. Sueoka, E. Sueoka, S. Matsuyama, K. Imai, K. Nakachi, and H. Fujiki. 1999. Green tea and cancer chemoprevention. *Mutat. Res.* 428:339.
- Yang, G. Y., J. Liao, K. Kim, E. J. Yurkow, and C. S. Yang. 1998. Inhibition of growth and induction of apoptosis in human cancer cell lines by tea polyphenols. *Carcinogenesis* 19:611.
- Liang, Y. C., S. Y. Lin-Shiau, C. F. Chen, and J. K. Lin. 1999. Inhibition of cyclin-dependent kinases 2 and 4 activities as well as induction of Cdk inhibitors p21 and p27 during growth arrest of human breast carcinoma cells by (-)-epigallocatechin-3-gallate. *J. Cell. Biochem.* 75:1.
- Lu, Y. P., Y. R. Lou, J. G. Xie, Q. Y. Peng, J. Liao, C. S. Yang, M. T. Huang, and A. H. Conney. 2002. Topical applications of caffeine or (-)-epigallocatechin gallate (EGCG) inhibit carcinogenesis and selectively increase apoptosis in UVB-induced skin tumors in mice. *Proc. Natl. Acad. Sci. USA* 99:12455.
- Yang, F., W. J. de Villiers, C. J. McClain, and G. W. Varilek. 1998. Green tea polyphenols block endotoxin-induced tumor necrosis factor-production and lethality in a murine model. *J. Nutr.* 128:2334.
- Dona, M., I. Dell'Aica, F. Calabrese, R. Benelli, M. Morini, A. Albini, and S. Garbisa. 2003. Neutrophil restraint by green tea: inhibition of inflammation, associated angiogenesis, and pulmonary fibrosis. *J. Immunol.* 170:4335.
- Lee, S., S. Suh, and S. Kim. 2000. Protective effects of the green tea polyphenol (-)-epigallocatechin gallate against hippocampal neuronal damage after transient global ischemia in gerbils. *Neurosci. Lett.* 287:191.
- Levites, Y., O. Weinreb, G. Maor, M. B. Youdim, and S. Mandel. 2001. Green tea polyphenol (-)-epigallocatechin-3-gallate prevents N-methyl-4-phenyl-1,2,3,6-tetrahydropyridine-induced dopaminergic neurodegeneration. *J. Neurochem.* 78:1073.
- Steinman, L. 2001. Multiple sclerosis: a two-stage disease. *Nat. Immunol.* 2:762.
- Brosnan, C. F., and C. S. Raine. 1996. Mechanisms of immune injury in multiple sclerosis. *Brain Pathol.* 6:243.
- Steinman, L. 1999. Assessment of animal models for MS and demyelinating disease in the design of rational therapy. *Neuron* 24:511.
- Trapp, B. D., J. Peterson, R. M. Ransohoff, R. A. Rudick, S. Mork, and L. Bo. 1998. Axonal transection in the lesions of multiple sclerosis. *N. Engl. J. Med.* 338:278.
- Bjartmar, C., J. R. Wujek, and B. D. Trapp. 2003. Axonal loss in the pathology of MS: consequences for understanding the progressive phase of the disease. *J. Neurol. Sci.* 206:165.
- Diestel, A., O. Aktas, D. Hackel, I. Hake, S. Meier, C. S. Raine, R. Nitsch, F. Zipp, and O. Ullrich. 2003. Activation of microglial poly(ADP-ribose)-polymerase-1 by cholesterol breakdown products during neuroinflammation: a link between demyelination and neuronal damage. *J. Exp. Med.* 198:1729.
- Zamvil, S. S., and L. Steinman. 2003. Diverse targets for intervention during inflammatory and neurodegenerative phases of multiple sclerosis. *Neuron* 38:685.
- Aktas, O., S. Waiczies, A. Smorodchenko, J. Dorr, B. Seeger, T. Prozorovski, S. Sallach, M. Endres, S. Brocke, R. Nitsch, and F. Zipp. 2003. Treatment of relapsing paralysis in experimental encephalomyelitis by targeting Th1 cells through atorvastatin. *J. Exp. Med.* 197:725.
- Lünemann, J. D., S. Waiczies, S. Ehrlich, U. Wendling, B. Seeger, T. Kamradt, and F. Zipp. 2002. Death ligand TRAIL induces no apoptosis but inhibits activation of human (auto)antigen-specific T cells. *J. Immunol.* 168:4881.
- Ullrich, O., A. Diestel, I. Eyupoglu, and R. Nitsch. 2001. Regulation of microglial expression of integrins by poly(ADP-ribose) polymerase-1. *Nat. Cell. Biol.* 3:1035.
- Savaskan, N. E., A. U. Brauer, M. Kuhbacher, I. Y. Eyupoglu, A. Kyriakopoulos, O. Ninnemann, D. Behne, and R. Nitsch. 2003. Selenium deficiency increases susceptibility to glutamate-induced excitotoxicity. *FASEB J.* 17:112.
- Dörr, J., S. Waiczies, U. Wendling, B. Seeger, and F. Zipp. 2002. Induction of TRAIL-mediated glioma cell death by human T cells. *J. Neuroimmunol.* 122:117.
- Suganuma, M., S. Okabe, M. Oniyama, Y. Tada, H. Ito, and H. Fujiki. 1998. Wide distribution of [³H](-)-epigallocatechin gallate, a cancer preventive tea polyphenol, in mouse tissue. *Carcinogenesis* 19:1771.

23. Chow, H. H., Y. Cai, D. S. Alberts, I. Hakim, R. Dorr, F. Shahi, J. A. Crowell, C. S. Yang, and Y. Hara. 2001. Phase I pharmacokinetic study of tea polyphenols following single-dose administration of epigallocatechin gallate and polyphenon E. *Cancer Epidemiol. Biomarkers Prev.* 10:53.
24. Barnes, P. J., and M. Karin. 1997. Nuclear factor- κ B: a pivotal transcription factor in chronic inflammatory diseases. *N. Engl. J. Med.* 336:1066.
25. Nitsch, R., I. Bechmann, R. A. Deisz, D. Haas, T. N. Lehmann, U. Wendling, and F. Zipp. 2000. Human brain-cell death induced by tumour-necrosis-factor-related apoptosis-inducing ligand (TRAIL). *Lancet* 356:827.
26. Hu, W. H., H. Johnson, and H. B. Shu. 1999. Tumor necrosis factor-related apoptosis-inducing ligand receptors signal NF- κ B and JNK activation and apoptosis through distinct pathways. *J. Biol. Chem.* 274:30603.
27. Wei, H., X. Zhang, J. F. Zhao, Z. Y. Wang, D. Bickers, and M. Lebowitz. 1999. Scavenging of hydrogen peroxide and inhibition of ultraviolet light-induced oxidative DNA damage by aqueous extracts from green and black teas. *Free Radical Biol. Med.* 26:1427.
28. Haqqi, T. M., D. D. Anthony, S. Gupta, N. Ahmad, M. S. Lee, G. K. Kumar, and H. Mukhtar. 1999. Prevention of collagen-induced arthritis in mice by a polyphenolic fraction from green tea. *Proc. Natl. Acad. Sci. USA* 96:4524.
29. Hilliard, B. A., N. Mason, L. Xu, J. Sun, S. E. Lamhamedi-Cherradi, H. C. Liou, C. Hunter, and Y. H. Chen. 2002. Critical roles of c-Rel in autoimmune inflammation and helper T cell differentiation. *J. Clin. Invest.* 110:843.
30. Wang, X., H. Luo, H. Chen, W. Duguid, and J. Wu. 1998. Role of proteasomes in T cell activation and proliferation. *J. Immunol.* 160:788.
31. Hinz, M., D. Krappmann, A. Eichten, A. Heder, C. Scheidereit, and M. Strauss. 1999. NF- κ B function in growth control: regulation of cyclin D1 expression and G₀/G₁-to-S-phase transition. *Mol. Cell Biol.* 19:2690.
32. Nam, S., D. M. Smith, and Q. P. Dou. 2001. Ester bond-containing tea polyphenols potently inhibit proteasome activity in vitro and in vivo. *J. Biol. Chem.* 276:13322.
33. MacMicking, J. D., D. O. Willenborg, M. J. Weidemann, K. A. Rockett, and W. B. Cowden. 1992. Elevated secretion of reactive nitrogen and oxygen intermediates by inflammatory leukocytes in hyperacute experimental autoimmune encephalomyelitis: enhancement by the soluble products of encephalitogenic T cells. *J. Exp. Med.* 176:303.
34. Pisters, K. M., R. A. Newman, B. Coldman, D. M. Shin, F. R. Khuri, W. K. Hong, B. S. Glisson, and J. S. Lee. 2001. Phase I trial of oral green tea extract in adult patients with solid tumors. *J. Clin. Oncol.* 19:1830.
35. Kira, J. 2003. Multiple sclerosis in the Japanese population. *Lancet Neurol.* 2:117.